Volume 17, Issue 4, 172532 (1-13)

Iranian Journal of Earth Science (IJES)

https://doi.org/10.57647/j.ijes.2025.16785

A red horizon underneath Damavand Volcano Quaternary pyroclastics in Polur area, Iran

Mohsen Ranjbaran*, Seyyed Mohammad Zamanzadeh

School of Geology, College of Science, University of Tehran, Tehran, Iran.

***Corresponding author:** m.ranjbaran@ut.ac.ir

Original Research

Received:
2024-02-06
Revised:
2024-03-13
Accepted:
2024-05-18
Published online:
2025-05-09
Published in issue:
2025-10-30

Abstract:

There is a red horizon immediately below the lavas of Damavand volcano, which has been considered as a palaeosol since 1970s, though highly debated in nature up to now the release of the geological map of the studied area in the???. However, the nature of this red horizon is still debated. In this study, a thorough field work has been performed to recognize the stratigraphic position of this red horizon in the area and 65 samples were gathered from both lavas and underneath supposed sedimentary beds to prepare thin sections for petrography studies. In addition, XRD analysis was carried out on six fine grained subsamples to determine the mineralogical composition of silt and clay sized sediments located under the lavas. The results show that volcanic rocks in the Polur area consist of two types of intermediate and basic lavas, whereas the red horizon is composed of highly oxidized volcanic ashes combined with glass tuff and altered pyroclastics. The dominant clay minerals in the altered pyroclastics include illite and chlorite. The formation of red horizon is a consequence of simultaneous deposition of fluvial clastic sediments (such as shales, sandstones, and limestone from older formations) and pyroclastic ash fall deposits and later alteration and oxidation of Fe-bearing minerals in both fluvial sediments and ash fall deposits. The results show that the red horizon which is seen underneath the lava deposits of the Damavand volcano in the Polur area should thus no longer be considered as a palaeosol. This is in contrast to most of previous studies in this area and worldwide.

Keywords: Damavand stratovolcano; Quaternary pyroclastics; Red horizon; Clay minerals; Iran

1. Introduction

The occurrence of red horizons under or within the lava flows has attracted many researchers who are enthusiastic about knowing the nature and development conditions of these “red horizons” since long time ago (e.g., (Emeleus et al., 1996); (Nanzyo, 2002); (Shikazono et al., 2005); (Lewis and Hampton, 2015); Solleiro-Rebolledo et al. (2015); Shomali and Shirzad (2015); Ghasempour et al. (2015); Melelli et al. (2017); Shamsi et al. (2019); Yamani et al. (2019); Ahmadi et al. (2020); Moradi et al. (2021); Irannezhadi et al. (2022), Rahimi et al. (2022), Rincón et al. (2023), Esmaili (2024); Niazpour and Shomali (2024); Elmi et al. (2025); Abdolahadi et al. (2025)). These red horizons sometimes were considered as paleosols and named as “boles” (Emeleus et al., 1996). In Iran, there is a famous red horizon underneath Damavand lavas which has been considered as a paleosol for many years since the first geological map of the area was drawn (Allenbach, 1966). However, its exact nature is still debated: some researchers believe in the presence of a red palaeosol below the lava flows (Yazdi et al., 2019; Majidinia, 2012; Ousta et al., 2024), whereas others stated that they are composed of pyroclastics under the lava flows (Pandamouz, 1998). In this study, we focus on a particular red horizon described at the southern edge of volcanic flows from the Damavand volcano (northern Iran). Consequently, this paper tries to solve this pending debate by documenting the conditions of formation, the texture and mineralogy of this red horizon and the overlying basal unit of the Damavand Quaternary lava sequence.

2. Geological setting

The area of interest is located in the Central Alborz Range about 70 km northeast of Tehran in Mazandaran province. In the Central Alborz two different structural trends intersect to form a special zone in the Alborz Mountain range (Ehteshami-Moinabadi and Nasiri, 2019). Our studied area is located in this zone at the southern foot of Damavand volcano near Polur village (Fig. 1).

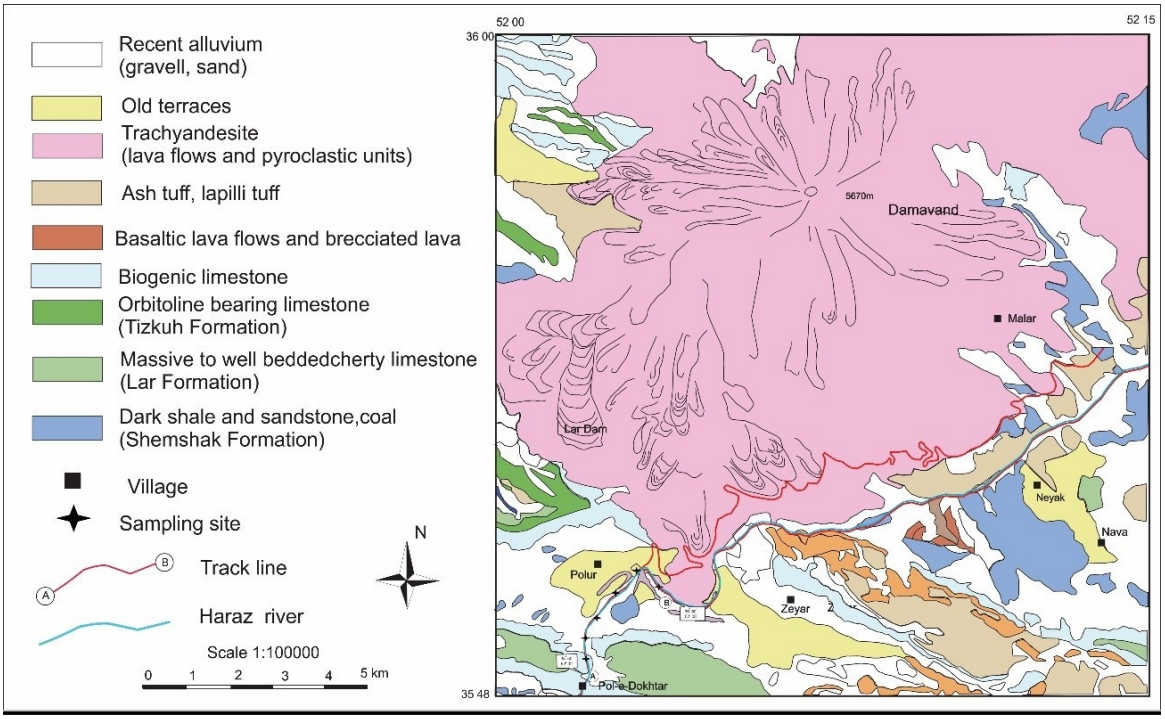

Figure 1. The geological location of Polur area: (a) Part of the central Alborz geological map showing the direction of lava flow towards South and West, and their relation to older rocks are shown (Allenbach and Steiger, 1972).

Culminating at 5671 m, the Damavand volcano is the highest mountain in the Western Asia and houses one of the highest glaciers in Iran (Williams and Ferrigno, 1991). This stratovolcano, which erupted over 400 km^2 of trachyandesite lava and pyroclastic deposits during the Quaternary, formed on the folded and faulted Alborz basement composed of older sedimentary deposits (Darvishzadeh, 1992). Its present shape is a huge complex cone owing to explosive and lava-bearing phases (Allenbach, 1966, 1970; Emami, 1992, 1989; Mortazavi and Sparks, 2011; Rahmani Javanmard et al., 2012) (Figs. 1 and 2). Its activity began during the Quaternary period, and two major eruption phases have been distinguished (Berzins et al., 2001). The eruptions of the Old Damavand phase began about 1.77 Ma and ceased about 544000 years ago, whereas those of the Young Damavand phase began about 445000 years ago and its last eruption was dated around 7300 years (Davidson et al., 2004). Mainly located on its northern flank, the oldest Damavand lava flows and pumices date back to 1.8 to 0.8 million years at the edge of the southwestern slope (Davidson et al., 2004). As for the youngest major activity phase, it resulted in huge deposits on the western flank only about 38000 years ago based on the radiometric dating of plant material in the underlying alluviums (Allenbach, 1970) and on apatite-based (U-Th)/He datings that yielded ages of about 7300 years (Davidson et al., 2004). The final morphological landscape of the Damavand peak was completed after its last eruption. Presently, the Damavand volcano is in the gas emission stage (Fig. 2).

Generally speaking, three distinct types of fall deposits can be distinguished in the Damavand area. Scoria type is simultaneous with the older eruption of basic lava flows activity and is composed of highly porous basaltic and andesitic fragments. The second and third types of fall deposits are respectively composed of pumice (rhyolitic) and ash (rhyolitic) deposits, which are simultaneous with the younger intermediate lava flows activity (Fig. 3 (a)). In the studied area, an alternating combination of scoria, pumice and ash fall deposits is always seen. This alternation starts with intermediate fall deposits and ends in basic ones (Moradi, 1996; Pandamouz, 1998; Mortazavi, 2017).

The Damavand volcano's lavas are covering Quaternary sediments and Mesozoic sedimentary formations, such as Elika (Triassic), Shemshak, Lar and Dalichai (Jurassic) formations. The general slope direction in the studied area is from the south to the north. As a result, the Haraz valley, which is resulted from the dynamics of the Haraz River, passes through the Alborz heights to the northern plains towards the Caspian Sea. Haraz River is an antecedent stream that was flowing towards the north before Damavand volcano eruptions started (Yamani et al., 2019). Indeed, before the eruption of the trachyandesites of Damavand, the Haraz River created an incised valley flowing towards the north into the Caspian Sea (Figs. 3 (a) and (b)). Drainage basin of the Haraz River, which is located along the eastern side of Damavand volcano, plays a fundamental role in modulating the topography of the volcano. This drainage basin is one of major south-to-north-flowing systems that cross the Alborz Mountains and flows into the Caspian Sea (Davidson et al., 2004). This river incised the older formations such as the Triassic Elika Formation (limestone), the Jurassic Shemshak (shale and sandstone), Lar and Dalichai formations (limestones) (Davidson et al., 2004). Later during Quaternary, fluvial-lacustrine sediments were deposited due to erosional/depositional activity of Haraz River (Moradi, 1996). In its later incising activity, the

Figure 2. South face view of the Damavand volcano peak.

river incised the latter fluvial-lacustrine deposits (Mozafari and Raeisi, 2017). Afterwards, this valley was filled in by the extruded trachyandesite lava flows moving over the river terraces to create a dam on the Haraz River. The accumulation of volcanic products from the Damavand volcano formed a lobe that forced the Haraz River to shift its course toward south and east of the volcano (Bashukooh, 2002; Yamani et al., 2019). However, the fluvial-volcanic deposits and even older formations are intersected in a few places by the Haraz valley (Fig. 4).

Previous field observations showed that the occurrence of two major eruption activity phases and several ash falls caused pyroclastic material to fall on the older rocks and sedimentary river deposits in many places in the south of the Damavand. The development of an underlying red horizon took place only at the boundary between lower (sedimentary) and upper (volcaniclastic) rocks. Furthermore, this red horizon crops out only near Polur village (Figs. 3 (b) and (c)) on the western bank of the Haraz River. It is not reported in other places in this area and it is most probably covered by Damavand lavas.

3. Material and methods

After a literature review and reconnaissance field work, along with using satellite images and geological maps of the Damavand 1:100000 and 1:250000 sheets, the study area was chosen. This study area includes a track line along the Haraz-Amol road 77 near Polur village in the Valley of Haraz River (Fig. 1). In the studied track, we proceeded to a stratigraphic survey including a drawing of the profile (without any scale), prepared a description of the stratigraphic

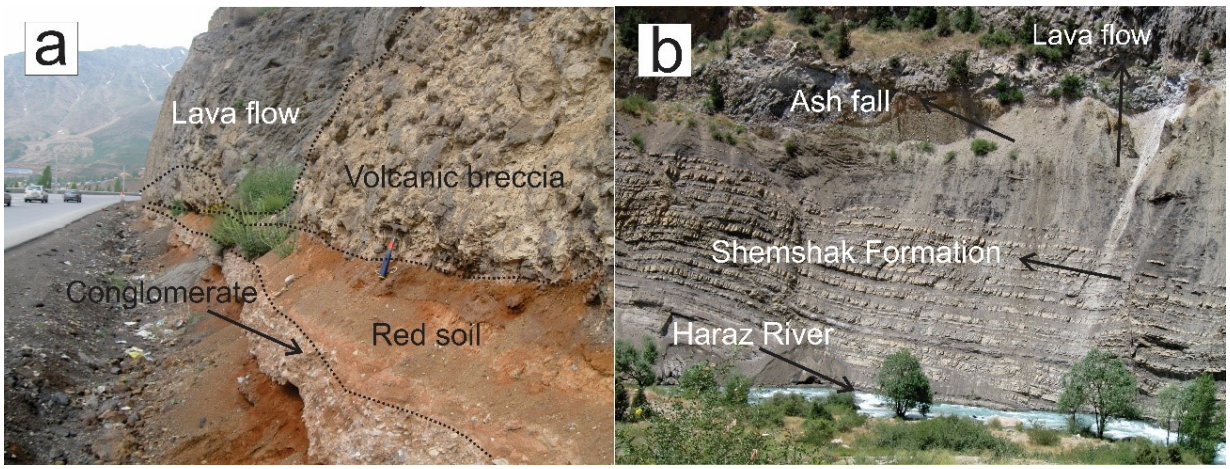

Figure 3. (a) From top to base lava flow, volcanic breccia, red soil and conglomerates and flood plain fine-grained deposits, (b) From top to base lava flow, ash fall, Shemshak Formation and Haraz River cuts through all lava flow, ash fall, Shemshak Formation.

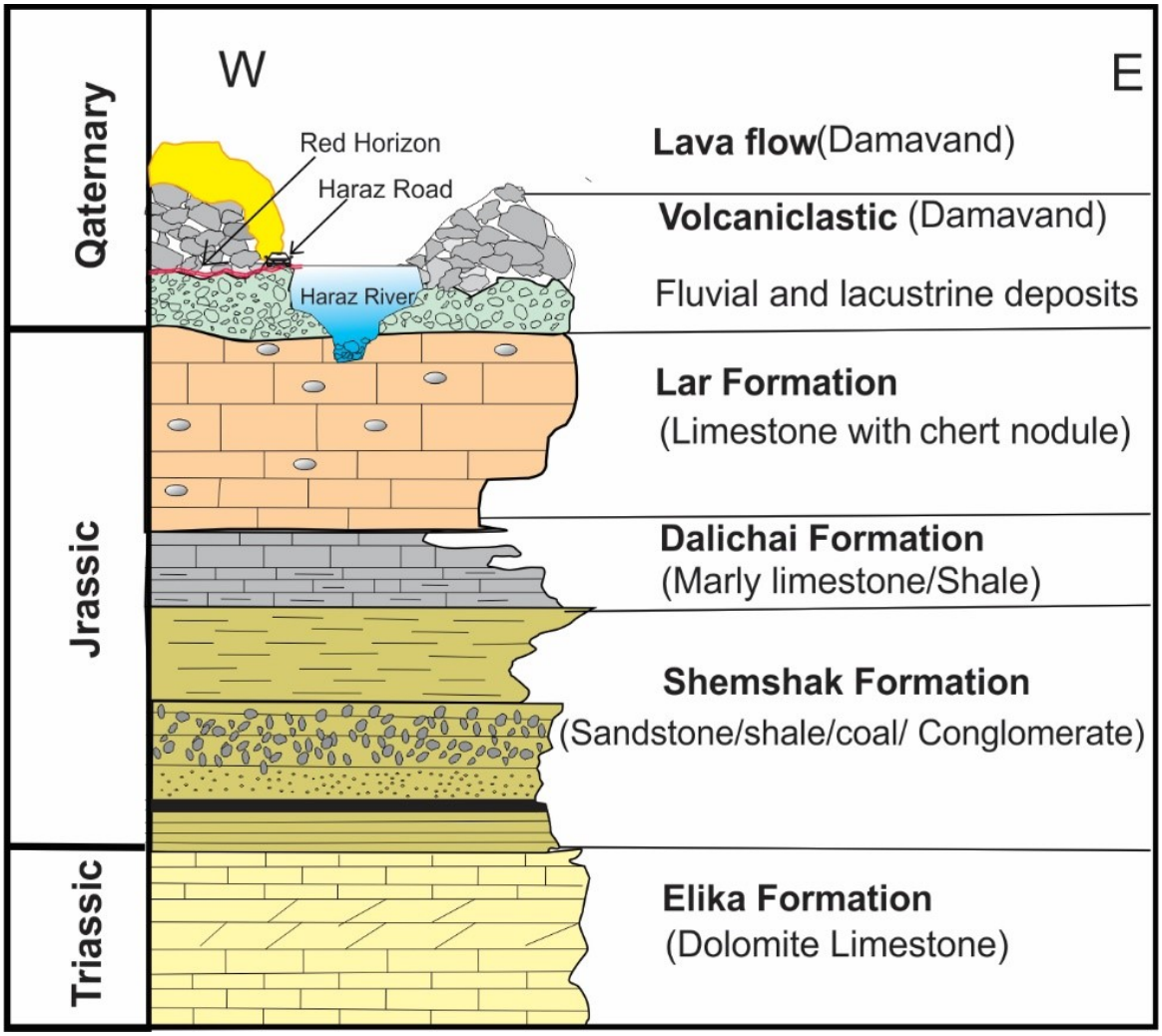

Figure 4. Schematic illustration representing the succession of formations and location of the red horizon under Damavand lavas along Haraz-Amol road (not to scale).

succession and descrided lithological/sedimentological characteristics of each unit.

In this track, near Polur village, we chose a succession of sedimentary-volcaniclastics and lava flows for sampling (samples: $16-22$, Table 1). Besides, we gathered some samples along this track at the sites where the texture and color of the rocks changed (samples: $1-15$, Table 1). Totally, we gathered 65 samples along this track for petrography and geochemical analysis (XRD and XRF). These samples were gathered from different units consisting of lavas, volcaniclastic sediments, the red horizon and lacustrine deposits underlying the red horizon. The information about description of the samples, their geographical location and codes are presented in Table 1. According to the profile presented in Fig. 5, the samples were taken from the base (Unit "A") to the top (Unit "F"). In this regard, six samples were taken from the base of the sequence up to the contact between lava and red horizon (one sample from each unit). In this study, 35 thin sections were prepared from all samples (several sample was taken from the same rock units for geochemical analysis) and petrographic studies were carried out on them. To study the mineralogical composition of the sediments lying under the lavas X-ray diffraction (XRD) was used. XRD analysis was carried out on six volcaniclastics, sediments and sedimentary rock samples from unit A to unit F respectively (Fig. 4). The XRD results are used to study the fine-grained parts, which are not distinguishable by optical microscopy (Eskandari et al., 2015; Eskandari et al., 2018). Thirteen samples from lava flows (unit F) and pyroclastic deposits (unit E) were chosen for geochemical analysis (XRF) which were carried out in the Iranian Geological Survey laboratory (Table 2).

4. Results

4.1 Field observations, sedimentary and petrographic analyses

The sedimentary-volcaniclastic sequence profile (in Polur area) is described below (Fig. 5).

As shown in Fig. 5 (a) total of 6 units nominated A to F were recognized in this area. In the outcrop, a distinct change in color separates mostly sedimentary red-brown units A to C, which are baked (i.e., slightly metamorphosed) from the overlying gray-black ash fall, volcanic breccia and lava flows (i.e. units D to F).

Unit "A" is a clastic conglomerate layer of fluvial sediments, including coarse-grained various rounded particles in the

Table 1. Location of sampling sites in Polur area.

Sample no.	Serial no.	(Thin-sections/geochemistry/XRD)	Sample name and description	Coordinates (Longitude-latitude)
1	MR.1	(thin-sections)	Clastic conglomerate layer	50° 03′ 43″ - 35° 50′ 32″
2	MR.2	(thin-sections)	Clastic conglomerate layer	50° 03′ 43″ - 35° 50′ 32″
3	MR.3	(thin-sections)	Clastic conglomerate layer	50° 03′ 43″ - 35° 50′ 52″
4	MR.4	(thin-sections/geochemistry)	Fine-grained volcanic	52° 03′ 43″ - 35° 50′ 52″
5	MR.5	(thin-sections/geochemistry)	Fine-grained volcanic	52° 03′ 06″ - 35° 50′ 52″
6	MR.6	(thin-sections/geochemistry)	Fine-grained volcanic	52° 03′ 06″ - 35° 50′ 52″
7	MR.7	(thin-sections/geochemistry)	Fine-grained volcanic	52° 03′ 06″ - 35° 50′ 52″
8	MR.8	(thin-sections/geochemistry)	Fine-grained volcanic	52° 03′ 06″ - 35° 50′ 52″
9	MR.9	(thin-sections/geochemistry)	Fine-grained volcanic	52° 03′ 06″ - 35° 50′ 52″
10	MR.10	(thin-sections/geochemistry)	Fine-grained volcanic	52° 03′ 06″ - 35° 50′ 52″
11	MR.11	(thin-sections/XRD)	Marl	52° 03′ 30″ - 35° 50′ 52″
12	MR.12	(thin-sections/XRD)	Marl	52° 03′ 30″ - 35° 51′ 16″
13	MR.13	(thin-sections/XRD)	Marl	52° 03′ 30″ - 35° 50′ 16″
14	MR.14	(thin-sections/geochemistry)	Basalt	52° 03′ 47″ - 35° 50′ 47″
15	MR.15	(thin-sections/geochemistry)	Basalt	52° 03′ 47″ - 35° 50′ 47″
16	MR.16	(thin-sections/XRD)	Red Horizon	52° 03′ 43″ - 35° 50′ 32″
17	Po.1	(thin-sections/XRD)	Red Horizon	52° 02′ 43″ - 35° 50′ 32″
18	Po.2	(thin-sections/XRD)	Red Horizon	52° 02′ 43″ - 35° 50′ 32″
19	Po.3	(thin-sections/XRD)	Red Horizon	52° 02′ 43″ - 35° 50′ 32″
20	Po.4	(thin-sections/XRD)	Red Horizon	52° 02′ 43″ - 35° 50′ 32″
21	Po.5	(thin-sections/XRD)	Red Horizon	52° 02′ 43″ - 35° 50′ 32″
22	Po.6	(thin-sections/XRD)	Red Horizon	52° 02′ 43″ - 35° 50′ 32″

lower part, in which some traces of volcanic fragments originated from the Damavand older eruptions can be seen. This conglomeratic unit has a channel fill geometry and represents a finning upward nature so that a fine-grained sandstone unit with an average thickness of 30 cm is observed on top this conglomerate. According to the petrography studies the constituent fragments of this conglomerate include some clasts from older sedimentary formations such as Lar (upper Jurassic limestone) and Shemshak (lower Jurassic shale/sandstone beds) formations as well as basaltic fragments originated from older volcanic rocks in a red clay matrix (Fig. 6 (a)). Unit “A” is interpreted as a river bed

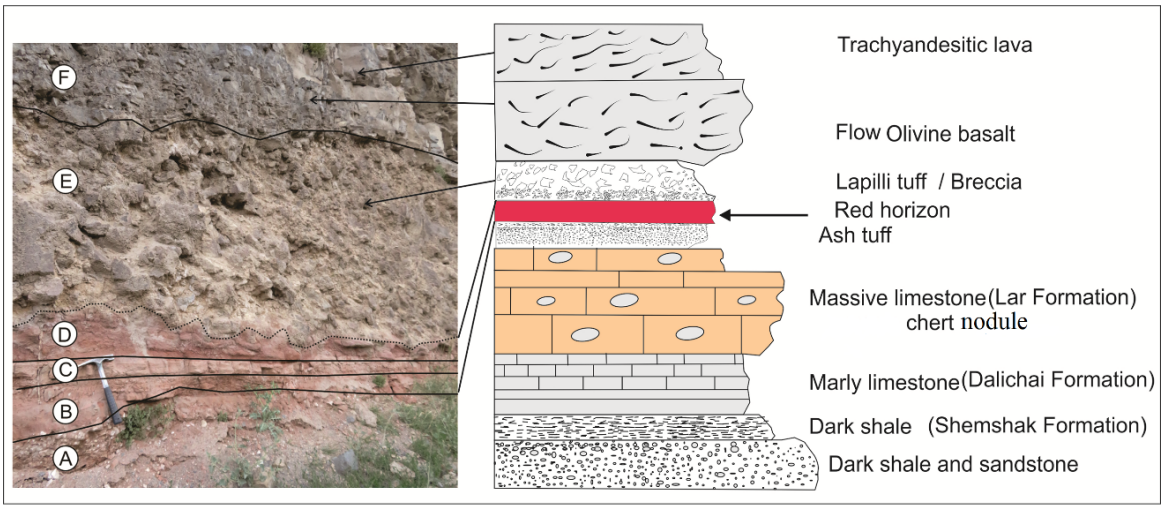

Figure 5. Sedimentary-volcaniclastic sequence profile along the Haraz Road (Road 77) at the western margin of the Haraz River valley in the Polur area. In this profile, six units are recognized and represented from “A” (base) to “F” (top), respectively.

Table 2. Approximate chemical composition of basaltic samples determined by XRF (Majidinia, 2012).

Sample	P01	P04	P10	P13	P17	P22	P25	P30	P34	P36	P37	P41	P42
Rock type	Trachy basalt				Basalt	Trachy basalt						Trachy Andesite	
Major Oxides (wt%)													
SiO_2	48.6	49.6	47.5	49.2	48.6	49.2	49.8	48.2	48	49.3	48.7	60	59.1
TiO_2	1.7	1.88	1.99	1.95	1.81	1.78	1.75	1.83	1.92	1.83	1.73	1.07	1.14
Al_2O_3	13.6	14	14.3	13.9	14.9	13.7	14.1	13.8	13.2	13.7	13.6	14.5	15.7
Fe_2O_3	2.85	3.01	3.06	3.1	2.87	3.09	3.02	3.03	3.01	3.18	3.06	2.24	2.3
FeO	5	5.07	5.37	5.13	5.5	5.29	5.28	5.36	5.04	5.25	5.03	6.64	2.66
MnO	.12	.12	.12	.13	.13	.13	.13	.13	.13	.13	.12	.07	.08
MgO	8.17	8.55	8.49	8.61	8.46	8.65	8.57	7.98	9.43	8.63	8.61	3.1	2.95
CaO	8.48	7.72	8.43	8.17	8.09	8.48	8.31	9.42	8.08	8.1	8.78	4.76	4.68
Na_2O	3.5	4	2.4	3.5	2.8	3.03	4.1	3.1	3.1	4.2	3.3	4.3	4.08
K_2O	1.77	1.37	2.87	2.29	1.75	2.15	1.26	2.18	2.01	1.63	1.87	3.88	4.16
P_2O_5	1.16	1.26	1.33	1.34	1.21	1.2	1.26	1.29	1.34	1.24	1.24	.68	.67
Fe_2O_3(Tot)	8.45	8.68	9.06	8.84	9.01	9.01	8.92	9.02	9.05	9.06	8.69	5.2	5.29
Feo(Tot)	7.59	7.80	8.14	7.94	8.09	8.09	8.01	8.1	8.13	8.014	7.08	4.67	4.75
Cr_2O_3	.03	.04	.04	.04	.03	.04	.04	.04	.04	.04	.04	$< .01$	$< .01$

channel filling conglomerate.

Unit B is a sedimentary unit with a finer texture than unit "A". This unit is seen as pale red sandstone with an almost lenticular geometry filling the channels on top of coarser grained conglomeratic unit (i.e., A). Unit "B" represents more textural uniformity with a fine-grained texture in comparison with unit "A". The sporadically scattered finer grains (feldspar grains and limestone litchis), which are cemented with a carbonate cement, include little rock debris (with andesitic composition) resulted from the Damavand explosion (Fig. 6 (b)). Unit "B" is mostly composed of a matrix of plagioclase fragments and well sorted and finer-grained rock debris (mostly shale and sandstone), as well as calcium carbonate cement (Fig. 6 (c)). This unit is interpreted as channel filling sandstone which is deposited as a result of waning river flows due to the abandonment of the river course.

Unit "C" includes a mixture of sedimentary and pyroclastic materials. It shows somehow blanket geometry. It is finer grained than previous unit and is represented by a red color. This unit is the red horizon which previously was considered as a palaeosol (Allenbach, 1966). Based on petrography study, this unit represents an intermediate combination of sedimentary (sandstone-siltstone) and volcaniclastic (andesitic-basaltic in composition) parts with negligible amounts of lithics from Lar Formation (limestone) and Shemshak Formation (shale and sandstone). The andesitic-basaltic lithics are slightly altered and represent a red color in the field. Formation of this unit is resulted from combination of both sedimentary and volcanic processes so that flood plain deposits (i.e., sandstone-siltstone) were intermingled with volcaniclastic materials.

Unit "D" is an ash fall tuff. The lower boundary of this unit is approximately horizontal but the upper boundary is uneven due to falling impact of large fragments of pyroclastic materials on these ash fall deposits. This unit has a blanket geometry in the study area. Based on the petrography studies, unit "D" is mainly composed of volcanic glass debris, among which some crystal fragments such as feldspar, biotite and, amphibole are observed. This is lithologically classified as glass tuff without pedogenesis evidence, i.e., highly oxidized glass tuff. The saturated porous spaces between glass fragments are filled with sparry calcite cement which is precipitated from meteoric infiltrating water coming through the upper units. The major mineralogical composition consists of pyroxene, amphibole, apatite crystals, all margins of which are oxidized (i.e., representing opacity), and glass (with flow texture) (Fig. 6 (d)). Oxidation margin of the Fe/Mg bearing minerals took place at the time of eruption. Feldspar crystals are mostly intact, so weathering (if happened) is insignificant. Deposition of this unit took place due to Damavand volcanic activity which resulted in settling of volcaniclastic materials as tuffs in a widespread manner on previous units. Unit "E" is observed in the field as a mixture of two volcanic (breccias) and sedimentary (marl) rocks. The first product consists predominantly of pyroclastic material, which is formed by the fall and flow from the Damavand eruption during the last phases. The second product comprises a soft deposit with a marl composition. According to petrography studies,

this unit is a mixture of two parts: carbonate mudstone and pyroclastic fragments. The former is micritic carbonate mud, with a silt-sized finely-grained microscopic texture (Fig. 6 (e)). The pyroclastic fragments are basaltic in composition and are vuggy and sometimes resemble scoria.
Within Polur lava flow, mudstone and micritic fragments are observed with fine-grained textures. During the lava movement, these fragments were plucked from lake floor sediments and mixed with lava. The lakes previously were formed due to the damming effect of lava flows in Haraz River it is interpreted that as a result of blocking the Haraz River flow by Damavand lava flows and formation of lakes behind this lava flows, marl deposition took place in the lake environments (Yamani et al., 2019). The formation of mudstone fragments was resulted from the crushing of carbonate rocks of older formations such as Dalichai (middle Jurassic) and Lar (upper Jurassic) and later deposition of the crushed grains as silt and fine-grained clay sediments. Occasionally pyroclastic fall materials are observed in the lakes deposits. The pyroclastic materials have fallen on the marly sediments; consequently, the predominant lithology is pyroclastic with minor fragments ($10-30$ cm) of marly sediments.
Unit "F" is a lava flow of trachybasaltic nature, covering all previous units. It is the thickest unit lying on top of the other units. It shows different features such as prismatic columns, degasing voids and amygdaloidal texture filled with calcite and zeolite minerals. Spheroidal weathering is sometimes observed in some parts in this unit (Fig. 7). Volcanic rocks in the Polur region are of two types: intermediate and basic. They were respectively resulted from the Old and Young Damavand activity phases. Based on petrographic studies, olivine and pyroxene (clinopyroxene) phenocrysts dominate over other crystals in basic rocks of the oldest eruptions (Emami, 1989, 1992; Majidinia, 2012; Yamani et al., 2019). In contrast, intermediate rocks of the youngest eruptions include pyroxene and sieve-textured plagioclase crystals (Assereto, 1966; Davidson et al., 2004). So generally speaking, these rocks have a microlithic porphyry texture with olivine, pyroxene and plagioclase minerals. Their voids and fractures were later filled with sparry calcite crystals (Fig. 6 (f)).

4.2 XRF and X-Ray Diffraction (XRD) studies

Since it is necessary to represent that the red horizon is not a weathering product of the volcaniclastics, we carried out XRD and geochemical analyses to find out the mineralogical composition of both the volcanclastics and the red horizon. Afterwards by comparing the results we can better understand whether there is a relationship between the volcaniclastics and the red horizon from mineralogical viewpoint or not. Based on the relationship between different volcanic tephra and their mineralogy, an estimate of probable mineral forms can be established for volcaniclastic deposits in a region (Shoji et al., 1993; Yamani et al., 2019) (Fig. 8). The XRD results revealed the presence of following minerals: Feldspar (dominant), calcite, quartz, muscovite, and hematite (Fig. 9). The diversity of minerals in Unit "A" is high compared to Unit "B." Therefore, the results of petrography study of volcaniclastics confirm the

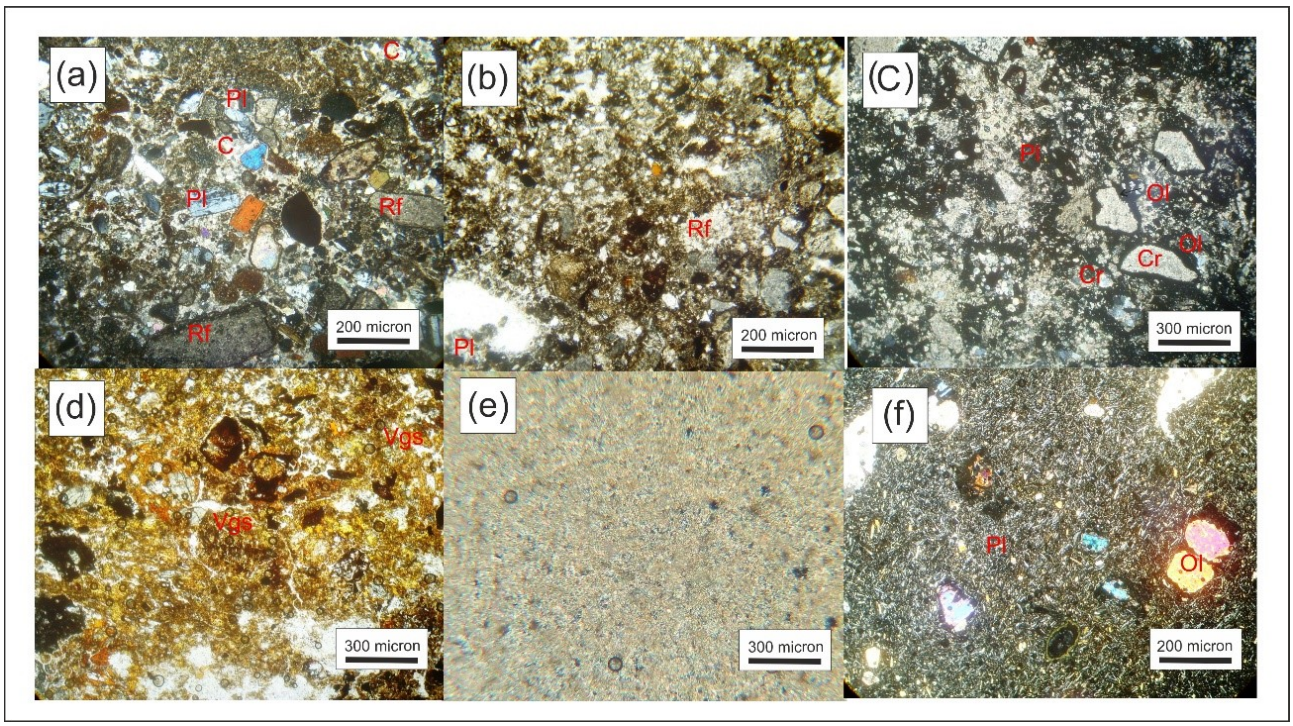

Figure 6. Microscopic images from the base to top of the volcaniclastic sequence (from Fig. 5): (a) this conglomerate is mostly composed of plagioclase(Pl) and rock fragments (Rf) (especially shale and sandstone) with calcite cement (C), (b) this sandstone has a fine grained texture and its composition is similar to unit (a) in lithology and finer crystalline calcium carbonate cement binds all these grains together; (c) this sample comprises a mixture of carbonate rock fragments (Cr) and porous volcanic lithics (Vl). Most of the grains have an oxidized margin (Om), probably due to the high temperature of lava and pyroclastic materials, (d) this tuff and breccia is composed of volcanic glass shards (Vgs) with porous appearance; (e) carbonate mudstone in plane-polarized light.; (f) olivine (Ol) basalt with Porphyry microlithic textures.

Figure 7. The Spheroidal weathering in lava flow with trachybasaltic composition, this type of physical weathering is the most prevalent erosion type in lava flows.

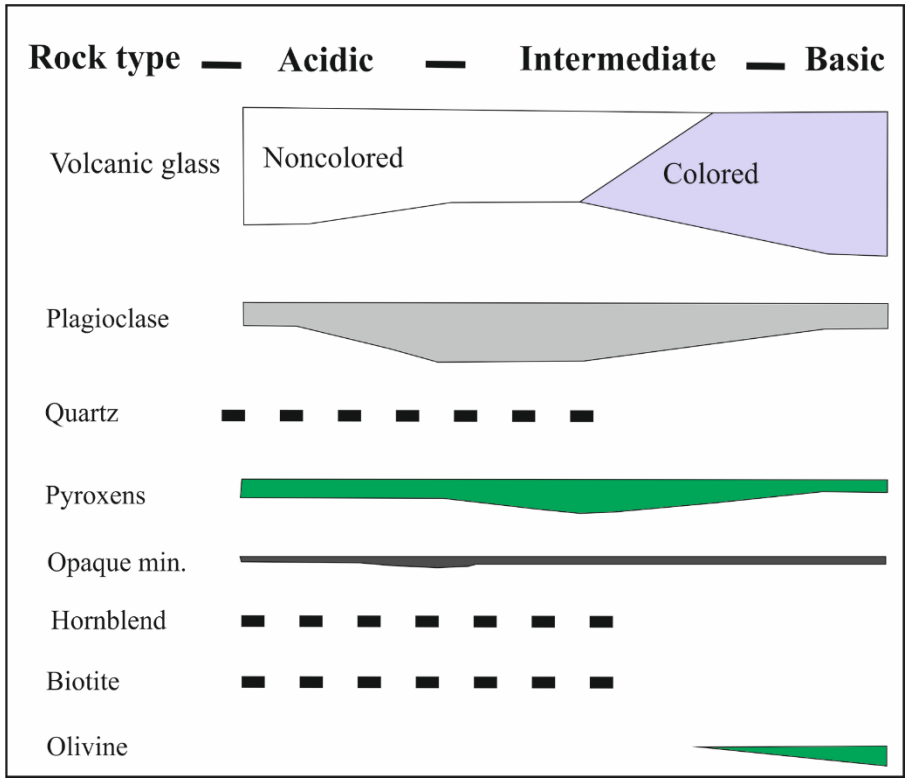

Figure 8. The relationship between different types of volcanic tephra and their mineralogy (Shoji et al., 1993).

intermediate composition of them.

Considering the results of XRD analysis and the absence of index clay minerals (such as illite and chlorite) in the diagrams, it seems that no significant alteration occurred within "A" to "C" units. This fact should be due to the lack of time for the young sediments to go through alterations which results in the formation of index clay minerals.

It should be mentioned that because it takes a long time to

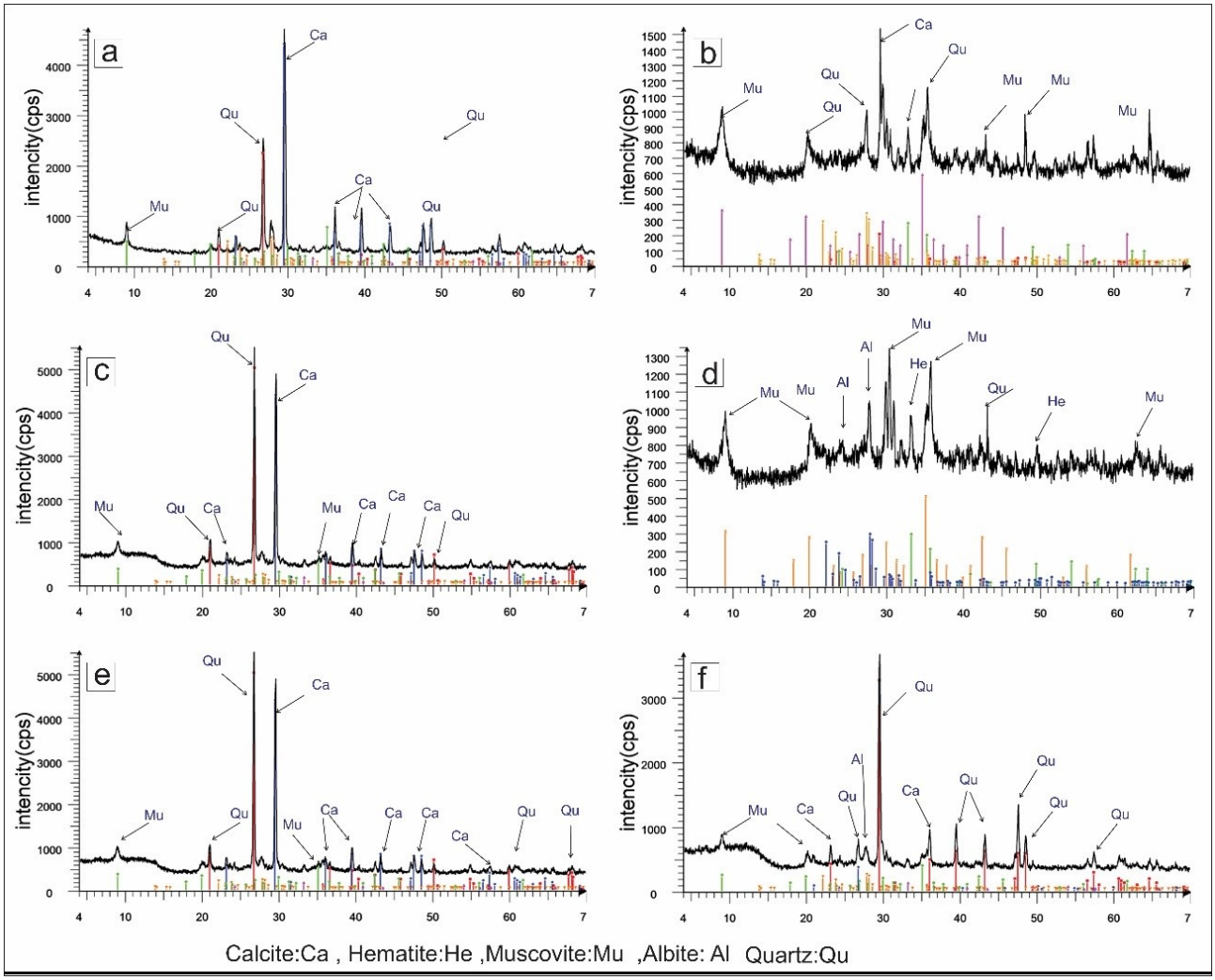

Figure 9. Six XRD patterns of samples of palaeosol and the deposits beneath pyroclastic fragments and lava in the Polur area; (a), (b), (c), (d), (e) and (f). Mg, Al, Ch, Qz, and Ca represent muscovite, albite, chlorite, quartz and calcite respectively.

form clay minerals resulting from decomposition, we do not see the presence of such minerals in the red horizon section. The most abundant clay mineral at the base of the sequence is illite, which is resulted from weathering of the Shemshak Formation shales (Jurassic). The Shemshak Formation is composed of both sandstone and shale beds. Petrographic studies show the presence of basaltic rocks in F unit.

For elaborating the type of igneous rock samples, we tried to use the results of geochemical analyses by plotting them in Total Alkaline Silica (TAS) and basalts classification diagram (Figs. 10 (a) and (b)). According to the TAS diagram (Middlemost, 1994), the results are mainly plotted in the trachybasalt field (Fig. 10 (a)). In this classification, the amount of silica (SiO_2) and alkalis ($Na_2O + K_2O$) were used. As it is seen in the latter diagram (Fig. 10 (a)) most of the results represent a trachybasaltic nature for the samples. Based on basalts classification diagram (Fig. 10 (b)) the results are mostly plotted in shoshonite series and some in high-K calc-alkaline fields. These results are in good accordance with previous studies carried out on Damavand lavas (Emami, 1989, 1992; Ranjbaran and Sotohian, 2020; Asadollah et al., 2018).

5. Discussion

In many parts of the world, there are some beds (mostly red-colored) composed of fine-grained sediments and clay minerals underlying lavas (Emeleus, 1985; Solleiro-Rebolledo et al., 2015). These red horizons are named “boles” if they are fossil lateritic soils and are the result of subaerial weathering of basaltic lavas under tropical conditions (Emeleus et al., 1996). However, sometimes these red horizons are developed below a lava flow due to a process called “rubefication” by hot lava (Emeleus et al., 1996). In the foothills of the Damavand volcano, there is a red horizon underlying Damavand Quaternary lavas and pyroclastics. This red horizon has long been considered as a palaeosoil due to its similarity in position below lavas like boles by many Iranian and international geologists (Davidson et al., 2004; Mortazavi and Sparks, 2011; Majidinia, 2012; Marques et al., 2014; Gürel and Özcan, 2016; Mortazavi, 2017).

Damavand pyroclastics are more voluminous than its lava flows, and are more visible in the southern, eastern and western parts compared to the northern parts (Darvishzadeh and Moradi, 1997; Yamani et al., 2019). The Damavand volcanic activity included a mixture of explosive and lava

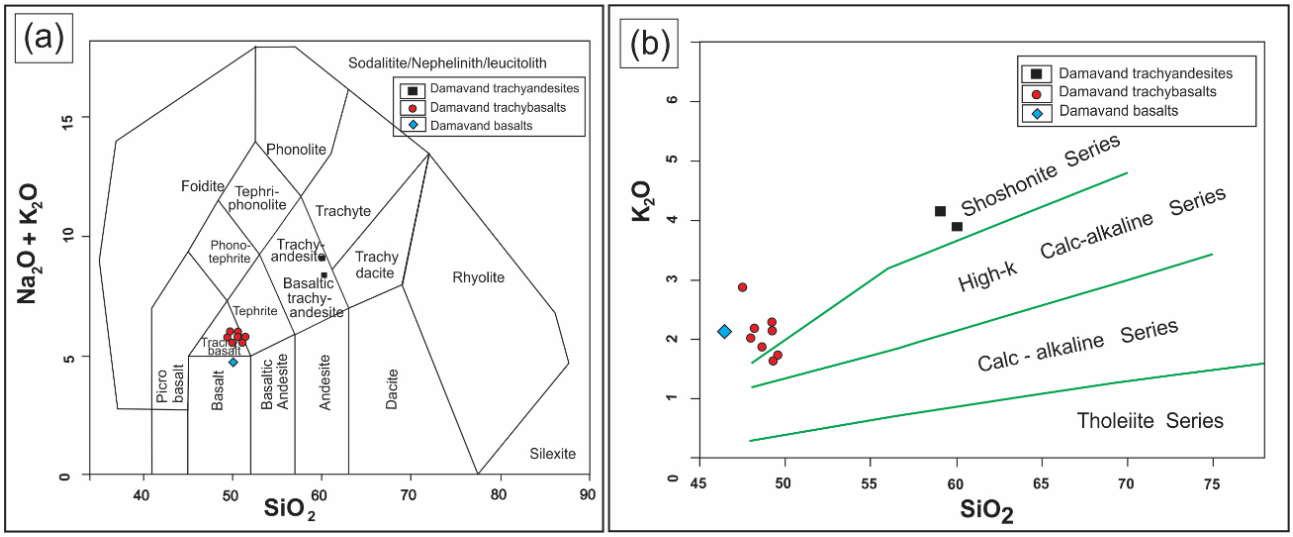

Figure 10. Chemical classification diagrams for the volcanic rocks over soils: (a) Total alkali versus silica (TAS) diagram (Middlemost, 1994), (b) K_2O versus SiO_2 diagram (Peccerillo and Taylor, 1976; Winchester and Floyd, 1977).

flows extrusion phases. The extrusion of lava flow blocked rivers such as Lar, Haraz and Dalichai Rivers in the west, south and southeastern part of the Damavand, creating some small local lakes followed by lacustrine sediments deposition and later lake terrace formation (Fig. 11) (Yamani et al., 2019).

While sediments were precipitated in such lakes, extrusive igneous activities with the andesitic-basaltic combination began with an intense explosion resulting in the entrance of porous fragments (andesitic in composition) and ash particles into these lakes. These activities resulted in an alternating deposition of lake sediments and pyroclastic materials (Fig. 12).

Sediments underlying the Damavand pyroclastics and lavas (i.e., the red horizon) represent a poor metamorphic aureole with a brick red color. The color variations towards the palaeo-surface (i.e., dark reddish brown, yellowish-brown to red and pale red) are mainly resulted from the color of the fine fraction of the various beds. Hematite is the main iron phase responsible for the color. This hematite staining is probably due to the thermal effect of the overlying hot volcanic unit (Marques et al., 2014; Solleiro-Rebolledo et al., 2015). According to our investigations, this red unit is not a palaeosol regardless of its resemblance to well-defined palaeosols in other parts of the world (e.g., Sayyed and Hundekari (2006), Sayyed (2014), Sayyed et al. (2014), and Gürel and Özcan (2016).

The main alteration processes of the ash deposits appear to be due to (i) weathering mechanisms and (ii) thermal metamorphism caused by the overlying lava contributing to reddening and cementation of the upper parts of the sedimentary units. Biological remains are absent either due to the palaeoenvironmental conditions or to the effect of heating. Since there are no biological remains in the sediments, it is plausible to consider the second mechanism (i.e., thermal metamorphism) to be responsible for the alteration of ash deposits and sediments and then reddening of them.

6. Conclusion

The goal of this research was to clarify whether the red horizon, which is underlying Damavand volcaniclastic rocks, is a palaeosol or not. A quick look at the Damavand sedimentary-volcanic sequence indicates that the lower part

Figure 11. Palaeo-lake deposits on the bank of Dalichai River.

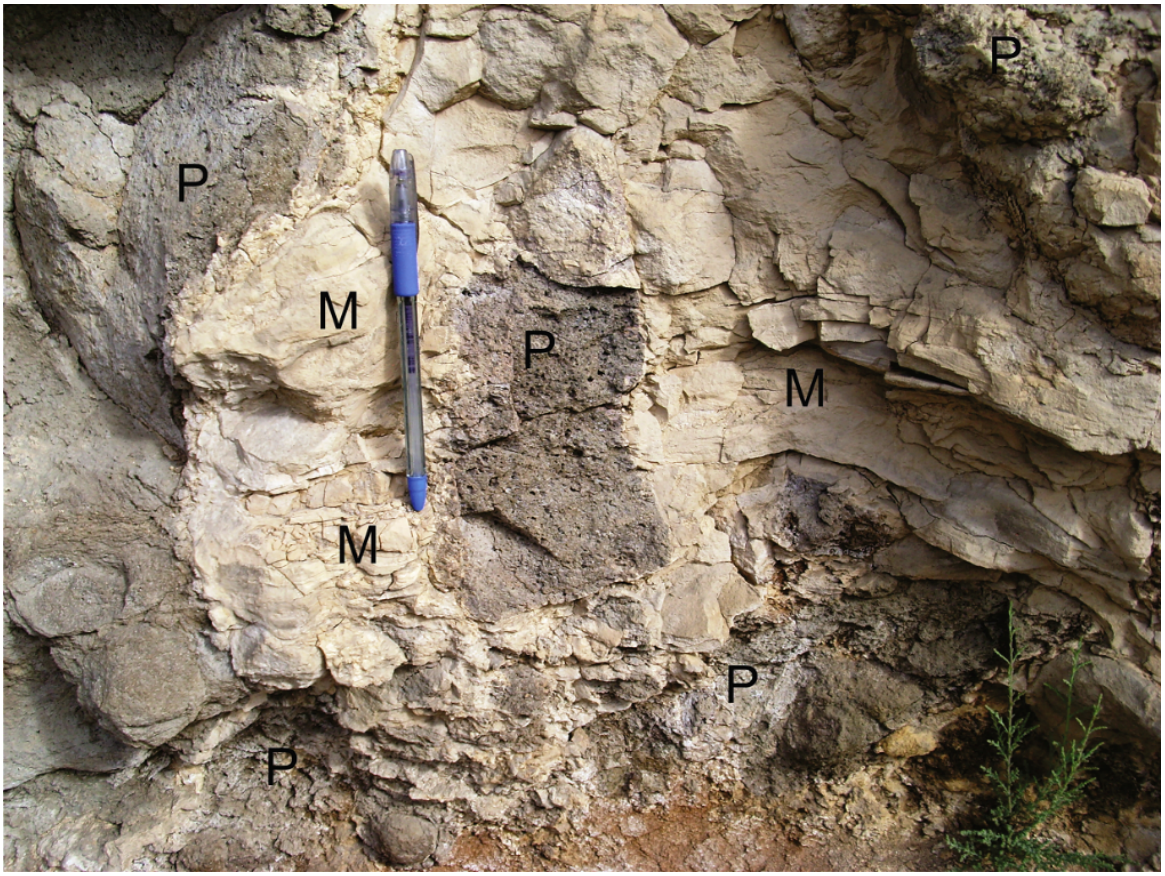

Figure 12. Unit "E" in Sedimentary-volcaniclastic sequence profile from Fig. 4. This unit consists of two parts. The pyroclastic material (P) and soft deposits with a marl composition (M) which surrounds pyroclastic materials.

of the sequence includes fluvial-lacustrine sediments above which a fine-grained sedimentary unit with some volcanic elements (e.g., ash and feldspar crystals) occurs. After this first volcanic ash fall, the glass tuff appears and this combination is later affected by thermal alterations and resulted in a false lateritic soil appearance. Above this part, the sediments are affected by the volcaniclastic materials and lava flows, which were lying on the upper part of this sequence.

The results of the microscopic studies on the red horizon show a variety of volcanic debris, e.g., feldspar, amphibole, biotite and pyroxene fragments, as well as lithics and basic volcanic glass debris. This diversity was originated from the type of falling ashes of the Damavand volcano. All of the above mentioned Fe/Mg minerals represent an oxidized (hematitic) rim which is the main reason for the red color of this horizon. The results of XRD analysis carried out on samples from the red horizon represent the dominance of illite mineral over the other clay minerals which are usually found in soil horizons. Based on petrographic and XRD analyses, illite was not a weathering product of volcaniclastics material during pedogenesis processes; rather it was derived from weathering of Shemshak Formation (Jurassic) shales. İn the latter shales, illite is the most abundant clay mineral.The effect of weathering in the red horizon is very weak. An evidence of this weak weathering is represented by intact feldspar crystals in this horizon.

Since the weathering effect in the red horizon, which is lying immediately under the pyroclastics and lava flows of Damavand in the Polur area, is very weak and minimal, so this red horizon is not a palaeosol; rather it is a mixture of fine-grained sediments along with glass tuff with palaeosol appearance. Earlier studies incorrectly mentioned that the red horizon is a palaeosol. The red color of this unit is due to the high temperature of lava, oxidizing the tuff deposits and further causing their brick red color resembling a lateritic horizon in the field. Consequently, according to the results of this study, it is suggested that the term red horizon is used instead of palaeosol in the Polur area where the only outcrops of this horizon are seen. Also if similar situation is encountered worldwide, the red horizons underneath lavas are suggested to be thoroughly studied and analyzed just to avoid possible long-lasting mistakes. and even in other palces if this red horizon is found and reported later.

Acknowledgement

The authors would like to acknowledge University of Tehran for supports in the field works.

Authors contributions
Authors have contributed equally in preparing and writing the manuscript.

Availability of data and materials
The data that support the findings of this study are available from the corresponding author, upon reasonable request.

Conflict of interests
The authors declare that they have no known competing financial interests or personal relationships that could have appeared to influence the work reported in this paper.

References

Abdolahadi A., Sheikhzakariaee S. J., Yazdi A., Mousavi S. Z. (2025) Plio-Quaternary Adakite Genesis and Post-collisional Processes: Whole Rock Constraints and Sr, Nd Isotopic Compositions in Alborz Magmatic Belt, Ardabil, Iran. *Journal of Mining and Environment* 16 (2): 737–765. DOI: https://doi.org/10.22044/jme.2024.14781.2801.

Ahmadi T., Ramesht M. H., Sponholz B., Safari A., Yamani M., Mohammadi A. (2020) Damavand, Anticyclone of the Heraz Basin. *Physical Geography Research Quarterly* 52 (2): 193–216.

Allenbach P. (1966) Geologie und Petrographie des Demavand und seiner Umgebung (Zentral- Elburz, Iran). Mitteilungen aus dem Geologischen Institut der Eidgenössischen Technischen Hochschule und der Universität Zürich:1–144.

——— (1970) Geology and Petrography of Damavand and its environment (Central Alborz) Iran. *Geological Survey of Iran Report, No. 17.*

Allenbach P., Steiger R. (1972) Central Alborz geological map (1:100,000). *Geological Survey of Iran*

Asadollah S. N., Aalianvari A., Hajialibeigi H. (2018) Role of geological structures in seepage from Lar dam reservoir. *Arabian Journal of Geosciences* 11 (20): 1–12. DOI: https://doi.org/10.1007/s12517-018-3967-7.

Assereto R. (1966) Geological map of upper Djadjerud and Lar valleys (central Elburz, Iran), 1:50.000, with explanatory notes. Pubblicazione Istituto di Geologia dell'Università di Milano. 86.

Bashukooh B. (2002) Hydrothermal alteration at east of Yakhar glacier and its role in evaluation of Damavand volcano Central Alborz. MSc, Department of Geology, Faculty of Science, University of Tehran. 106.

Berzins R., Davidson J., Hassanzadeh J., Stockli D. F., Bashukooh B., et al. (2001) Damavand Volcano, Northern Iran: Morphology and Sedimentary Record. GSA Annual Meeting, Boston, Massachusetts.

Darvishzadeh A. (1992) *Geology of Iran* Neda Publication

Darvishzadeh A., Moradi M. (1997) Fall differentiation in pyroclastic fall deposits of Damavand Volcano. *Journal of Science* 23:31–46.

Davidson J., Hassanzadeh J., Berzins R., Stockli D. F., Bashukooh B., Turrin B., Pandamouz A. (2004) The geology of Damavand volcano, Alborz Mountains, northern Iran. *Geological Society of America Bulletin* 116:16–29. DOI: https://doi.org/10.1130/B25344.1.

Ehteshami-Moinabadi M., Nasiri S. (2019) Geometrical and structural setting of landslide dams of the Central Alborz: a link between earthquakes and landslide damming. *Bulletin of Engineering Geology and the Environment* 78 (1): 69–88. DOI: https://doi.org/10.1007/s10064-017-1021-8.

Elmi R., Arian M. A., Ashja Ardalan A., Yazdi A. (2025) Petrology of volcanism in the Alasht-Haraz road of the Alborz mountain range, south of Amol (north of Iran). *Iranian Journal of Earth Sciences* 17 (3) DOI: https://doi.org/10.57647/j.ijes.2025.16800.

Emami M. H. (1989) Damavand Volcano and its Probable Activity. *Geological Survey of Iran, No. 559*

——— (1992) Damavand Volcano and its probable activity, Phase (1): Petrogenesis and magmatic evolution of Damavand volcano. International Institute of Earthquake Engineering and Seismology (HEES):71–92.

Emeleus C. H. (1985) The Tertiary lavas and sediments of northwest Rhum, Inner Hebrides. *Geological Magazine* 122 (5): 419–437.

Emeleus C. H., Cheadle M. J., Hunter R. H., Upton B. G. J., Wadsworth W. J. (1996) The Rum layered suite. *Developments in Petrology* 15:403–439.

Eskandari A., Amini S., Masoudi F. (2018) Monitoring thermal changes of Damavand Volcano using Landsat images. *Scientific Quarterly Journal Geosciences* 109 (28): 43–54. DOI: https://doi.org/10.22071/GSJ.2017.93384.1212.

Eskandari A., De Rosa R., Amini S. (2015) Remote sensing of Damavand volcano (Iran) using Landsat imagery: Implications for the volcano dynamics. *Journal of Volcanology and Geothermal Research* 306:41–57. DOI: https://doi.org/10.1016/j.jvolgeores.2015.10.001.

Esmaili R. (2024) Quantitative Evaluation and Spatial Clustering of Geodiversity in Iran. *Geoheritage* 16 (1): 13. DOI: https://doi.org/10.1007/s12371-024-00914-4.

Ghasempour M. R., Ghazi J. M., Biabangard H., Dabiri R. (2015) Petrogenic significance of the Plio-Quaternary Nehbandan mafic lavas, Eastern Iran. *Iranian Journal of Earth Sciences* 6 (2): 133–141.

Gürel A., Özcan S. (2016) Paleosol and dolocrete associated clay mineral occurrences in siliciclastic red sediments of the Late Miocene Kömişini Formation of the Tuzgölü basin in central Turkey. *Catena* 143:102–113.

Irannezhadi M. R., Ghorbani M. R., Hoernle K. A., Tavakoli N., Namnabat E., Hauff F., Hansteen T. (2022) Geochemistry and petrogenesis of tertiary subvolcanics from north Tehran, southern Central Alborz (Iran). *Arabian Journal of Geosciences* 15 (4): 331. DOI: https://doi.org/10.1007/s12517-022-09604-3.

Lewis G. M., Hampton S. J. (2015) Visualizing volcanic processes in Sketch Up: An integrated geo-education tool. *Computers & Geosciences* 81:93–100. DOI: https://doi.org/10.1016/j.cageo.2015.05.003.

Majidinia R. (2012) Petrology and geochemistry of the lavas in the Plour area and their flow mechanism. MSc, Department of Geology, Faculty of Science, University of Tehran, 95p. (in Persian with English abstract).

Marques R., Prudêncio M. I., Waerenborgh J. C., Rocha F., Dias M. I., Ruiz F., Muñoz A. M. (2014) Origin of reddening in a paleosol buried by lava flows in Fogo island (Cape Verde). *Journal of African Earth Sciences* 96:60–70. DOI: https://doi.org/10.1016/j.jafrearsci.2014.03.019.

Melelli L., Vergari F., Liucci L., Del Monte M. (2017) Geomorphodiversity index: Quantifying the diversity of landforms and physical landscape. *Science of the Total Environment* 584:701–714.

Middlemost E. A. (1994) Naming materials in the magma/igneous rock system. *Earth-Science Reviews* 37 (3-4): 215–224. DOI: https://doi.org/10.1016/0012-8252(94)90029-9.

Moradi A., Maghsoudi M., Moghimi E., Yamani M., Rezaei N. (2021) A Comprehensive Assessment of Geomorphodiversity and Geomorphological Heritage for Damavand Volcano Management, Iran. *Geoheritage* 13 (2): 23. DOI: https://doi.org/10.1007/s12371-021-00551-1.

Moradi M. (1996) Tephrochronology and eruption dynamics of Damavand volcano (Central Elborz, North of Iran).

Mortazavi M. (2017) High Potash Volcanic Rocks and Pyroclastic Deposits of Damavand Volcano, Iran, an Example of Intraplate Volcanism. *Journal of Sciences, Islamic Republic of Iran* 28 (2): 155–168.

Mortazavi M., Sparks R. S. J. (2011) Using Wind Data to Predict the Risk of Volcanic Eruption: An Example from Damavand Volcano, Iran. *Iranian Journal of Earth Sciences* 3:127–133.

Mozafari M., Raeisi E. (2017) Leakage paths at the Lar Dam site, northern Iran. Quarterly *Journal of Engineering Geology and Hydrogeology* 50:444–453. DOI: https://doi.org/10.1144/qjegh2017-016.

Nanzyo M. (2002) Unique properties of volcanic ash soils. *Global Environmental Research* 6 (2): 99–112.

Niazpour B., Shomali Z. H. (2024) Moderate earthquakes striking Tehran metropolitan area: a case study of 2017 Malard and 2020 Damavand seismic sequences. *Journal of Seismology* 28 (1): 103–117. DOI: https://doi.org/10.1007/s10950-023-10187-z.

Ousta S. H., Ashja-Ardalan A., Yazdi A., Dabiri R., Arian M. A. (2024) Petrogenesis and tectonic implications of Miocene dikes in the southeast of Bam (SE Iran): Constraints on the development of active continental margin. *Geopersia* 14 (1): 89–111. DOI: https://doi.org/10.22059/geope.2023.364334.648729.

Pandamouz A. (1998) A new investigation of the stratigraphic position of the basaltic flows in the volcanic sequence of Damavand (Central Albourz, N. Iran). MSc, Department of Geology, Faculty of Science, University of Tehran (in Persian with English abstract).

Peccerillo A., Taylor S. R. (1976) Geochemistry of Eocene calc-alkaline volcanic rocks from the Kastamonu area, Northern Turkey. *Contributions to Mineralogy and Petrology* 58:63–81.

Rahimi M., Zamani A., Ghotbi A. R. (2022) The study of seismicity of Alborz (Northern Iran) and Zagros (Southern Iran) regions by using time series analysis. *Acta Geophysica* 70 (1): 27–37.

Rahmani Javanmard S., Tutti F., Omidian S., Ranjbaran M. (2012) Mineralogy and stable isotope geochemistry of the Ab Ask travertines in Damavand geothermal field, Northeast Tehran, Iran. *Central European Geology* 55 (2): 187–212. DOI: https://doi.org/10.1007/s11600-021-00701-7.

Ranjbaran M., Sotohian F. (2020) Development of the Haraz Road geotourism as a key to increasing tourism industry and promoting geoconservation. *Geopersia* 11 (1): 61–79.

Rincón M., Márquez A., Herrera R., Martín-González F., López I., Crespo-Martín C. (2023) Morpho-structural criteria for the identification of spreading-induced deformation processes potentially compromising stratovolcano stability. *Bulletin of Volcanology* 85 (3): 17.

Sayyed M. R. G. (2014) Flood basalt hosted palaeosols: Potential palaeoclimatic indicators of global climate change. *Geoscience Frontiers* 5 (6): 791–799. DOI: https://doi.org/10.1016/j.gsf.2013.08.005.

Sayyed M. R. G., Hundekari S. M. (2006) Preliminary comparison of ancient bole beds and modern soils developed upon the Deccan volcanic basalts around Pune (India): Potential for palaeoenvironmental reconstruction. *Quaternary International* 156:189–199. DOI: https://doi.org/10.1016/j.quaint.2006.05.030.

Sayyed M. R. G., Pardeshi R. G., Islam R. (2014) Palaeoweathering characteristics of an intra-basaltic red bole of the Deccan Flood Basalts near Shrivardhan of western coast of India. *Journal of Earth System Science* 123 (7): 1717–1728.

Shamsi A., Karami G. H., Hunkeler D., Taheri A. (2019) Isotopic and hydrogeochemical evaluation of springs discharging from high-elevation karst aquifers in Lar National Park, northern Iran. *Hydrogeology Journal* 27 (2): 655–667.

Shikazono N., Suzuki C., Kitamura S., Watanabe H., Tano S., Tanaka A. (2005) Analysis of mutations induced by carbon ions in Arabidopsis thaliana. *Journal of Experimental Botany* 56 (412): 587–596.

Shoji S., Nanzyo M., Dahlgren R. A. (1993) Volcanic Ash Soils Genesis, properties and utilization. *Developments in Soil Science* 21:288.

Shomali Z.H., Shirzad T. (2015) Crustal structure of Damavand volcano, Iran, from ambient noise and earthquake tomography. *Journal of Seismology* 19:191–200.

Solleiro-Rebolledo E., Sedov S., Cabadas-Báez H. (2015) Use of soils and palaeosols on volcanic materials to establish the duration of soil formation at different chronological scales. *Quaternary International* 376:5–18.

Williams R. S., Ferrigno J. G. (1991) Glaciers of the Middle East and Africa. USGS Report, No. G1-G70.

Winchester J. A., Floyd P. A. (1977) Geochemical discrimination of different magma series and their differentiation products using immobile elements. *Chemical Geology* 20:325–343.

Yamani M., Moghimi E., Goorabi A., Zamanzadeh S. M., Mohamadi A. (2019) The relationship of the last Damavand eruptions and the sequence of lava barrage lakes. *Quantitative Geomorphological Research* 7 (3): 196–215.

Yazdi A., Ashja-Ardalan A., H. Emami M., Dabiri R., Foudazi M. (2019) Magmatic interactions as recorded in plagioclase phenocrysts of quaternary volcanics in SE Bam (SE Iran). *Iranian Journal of Earth Sciences* 11 (3): 215–225. DOI: https://doi.org/10.30495/ijes.2019.667379.